Contribution from the Institut für Physikalische und Theoretische Chemie and Physikalisches Institut, Abt. II, University of Erlangen-Nürnberg, D-8520 Erlangen, West Germany, and the Istituto di Chimica Generale e Inorganica, University of Florence, I-50132 Florence, Italy

Nature of the Continuous High-Spin ($^5T_2$) ⇌ Low-Spin ($^1A_1$) Transition in the Acetone Solvate of Dichlorobis[*cis*-1,2-bis(diphenylphosphino)ethylene]iron(II). Coupling with the Order–Disorder Transition of Acetone Molecules

E. KÖNIG,*[1a] G. RITTER,[1b] S. K. KULSHRESHTHA,[1a,c] J. WAIGEL,[1b] and L. SACCONI[2]

Received September 7, 1983

The gradual high-spin ($S = 2$; $^5T_2$) ⇌ low-spin ($S = 0$; $^1A_1$) transformation in solid $[Fe(dppen)_2Cl_2]\cdot 2(CH_3)_2CO$ (dppen = *cis*-1,2-bis(diphenylphosphino)ethylene) has been studied by variable-temperature ^{57}Fe Mössbauer effect and X-ray diffraction. The ground states involved are characterized, at the transition temperature $T_c \simeq 240$ K, by the quadrupole splittings $\Delta E_Q(^5T_2) = 2.63$ mm s^{-1} and $\Delta E_Q(^1A_1) = 0.66$ mm s^{-1} and the isomer shift $\delta^{IS}(^5T_2) = +0.82$ mm s^{-1} and $\delta^{IS}(^1A_1) = +0.41$ mm s^{-1}. The observed nonlinear temperature dependence of $-\ln(\sum t_i)$ where t_i is the effective thickness ($i = {}^5T_2$, $^1A_1$) provides evidence for different Debye–Waller factors, $-\ln f_{^5T_2}$ and $-\ln f_{^1A_1}$, the characteristic Mössbauer temperatures being $\Theta^M_{^5T_2} = 138$ K and $\Theta^M_{^1A_1} = 173$ K. The lattice spacings d_{hkl} derived from X-ray diffraction show a continuous shift with temperature due to the volume change associated with the spin transition. The results are consistent with the assumption of a weak cooperative interaction between the individual complexes and a wide distribution of the nuclei of the minority phase. The line widths in the Mössbauer spectra exhibit an unusual increase at $T_c^{acetone} \simeq 240$ K, additional anomalies being observed for the quantities $\Delta E_Q(^5T_2)$, $t_{^5T_2}/t_{total}$, and $-\ln(\sum t_i)$. The phenomenon is attributed to an order–disorder transition of the acetone molecule, which results in changes of the iron–phosphorus ligation. The two slightly different iron sites observed in the Mössbauer effect below $T_c^{acetone}$ thus correspond to two different orientations of the acetone molecule.

Recent studies have demonstrated that there exists a fundamental difference between the two types of high-spin ⇌ low-spin transitions:

Discontinuous type high-spin ⇌ low-spin transitions arise for compounds with a strong cooperative interaction between the individual complexes. In the transition region, pronounced domain formation by both the minority and the majority phases are encountered and, therefore, individual X-ray diffraction patterns for the two phases are observed.[3-6] Due to the interaction and domain formation, the transition is completed within a narrow temperature range and is associated, in general, with a crystallographic phase change. Hysteresis effects, whenever observed, are a consequence of the domain formation.

Continuous type high-spin ⇌ low-spin transitions show no individual X-ray diffraction patterns for the two spin constituents. Rather, the interplanar spacings d_{hkl} show a continuous variation with temperature, which conforms, in general, to that of the high-spin fraction n_{HS}.[7,8] These findings have been interpreted by the formation of a random solid solution of the two spin isomers within the same lattice. The continuous spin change is consistent with a weak cooperative interaction between the individual complexes and a wide distribution of the nuclei of the minority constituent. The continuous high-spin ⇌ low-spin transitions that have been investigated in greater detail are confined thus far to the iron(II) complexes $[Fe(bts)_2(NCS)_2]$, where bts = 2,2′-bi-5-methyl-2-thiazoline,[7] and $[Fe(4\text{-}paptH)_2]X_2\cdot 2H_2O$, X = ClO_4, BF_4, where 4-paptH = 2-((4-methyl-2-pyridyl)amino)-4-(2-pyridyl)thiazole.[8] In order to test the general applicability of the above interpretation, it is of importance to consider additional systems that display spin transitions of the continuous type.

The iron(II) complexes of the ligand dppen (=*cis*-1,2-bis(diphenylphosphino)ethylene) were studied for the first time by Levason et al.[9] It was established that $[Fe(dppen)_2Cl_2]$ shows a high-spin ($^5T_2$) ⇌ low-spin ($^1A_1$) transition, the system being almost completely in the high-spin state ($S = 2$; $^5T_2$) at 293 K, to somewhat less than 50% in the low-spin state ($S = 0$; $^1A_1$) at 195 K, and to more than 50% in the low-spin state at 77 K. More recently, one of the present authors[10] has performed detailed magnetic susceptibility measurements on two different polymorphs and several solvates of the $[Fe(dppen)_2Cl_2]$ complex. Of particular interest are the results obtained for the acetone solvate, $[Fe(dppen)_2Cl_2]\cdot 2(CH_3)_2CO$, since the effective magnetic moment decreases continuously from $\mu_{eff} = 5.11$ μ_B at 362 K to $\mu_{eff} = 0.69$ μ_B at 86 K, the larger part of the decrease taking place over a small temperature interval around 235 K. On the basis of these results, the spin transition seems to be almost complete at both temperature ends. In addition, single-crystal X-ray structure investigations were performed at both 295 and 130 K. According to this study,[10] the compound crystallizes in space group $P2_1/a$ with $Z = 2$, the metal atom being coordinated by two Cl atoms and by the four P atoms of the two dppen ligands in a trans-octahedral arrangement. The Fe atom lies rigorously in the plane of the four P atoms, the Fe–Cl bond forming an angle of ca. 7° with the normal to that plane. In the course of the spin transition, the average Fe–P bond distance decreases from 2.584 Å in the high-spin isomer (at 295 K) to 2.301 Å in the low-spin isomer (at 130 K). The change of about 0.28 Å is considerably larger than any variation in the metal–ligand bond length on spin transition previously reported, viz. 0.20 Å for Fe–N bonds.[11-13] The corresponding

(1) (a) Institut für Physikalische und Theoretische Chemie, University of Erlangen-Nürnberg. (b) Physikalisches Institut, Abt. II, University of Erlangen-Nürnberg. (c) On leave of absence from Bhabha Atomic Research Center, Bombay 400 085, India.
(2) University of Florence.
(3) König, E.; Ritter, G.; Irler, W.; Goodwin, H. A. *J. Am. Chem. Soc.* **1980**, *102*, 4681.
(4) König, E.; Ritter, G.; Irler, W.; Nelson, S. M. *Inorg. Chim. Acta* **1979**, *37*, 169.
(5) König, E.; Ritter, G.; Irler, W. *Chem. Phys. Lett.* **1979**, *66*, 336.
(6) König, E.; Ritter, G.; Kulshreshtha, S. K.; Nelson, S. M. *Inorg. Chem.* **1982**, *21*, 3022.
(7) König, E.; Ritter, G.; Kulshreshtha, S. K.; Nelson, S. M. *J. Am. Chem. Soc.* **1983**, *105*, 1924.
(8) König, E.; Ritter, G.; Kulshreshtha, S. K.; Goodwin, H. A. *Inorg. Chem.* **1983**, *22*, 2518.
(9) Levason, W.; McAuliffe, C. A.; Khan, M. M.; Nelson, S. M. *J. Chem. Soc., Dalton Trans.* **1975**, 1778.
(10) Cecconi, F.; Di Vaira, M.; Midollini, S.; Orlandini, A.; Sacconi, L. *Inorg. Chem.* **1981**, *20*, 3423.
(11) König, E.; Watson, K. J. *Chem. Phys. Lett.* **1970**, *6*, 457.
(12) Katz, B. A.; Strouse, C. E. *J. Am. Chem. Soc.* **1979**, *101*, 6214.
(13) Mikami, M.; Konno, M.; Saito, Y. *Acta Crystallogr., Sect. B: Struct. Crystallogr. Cryst. Chem.* **1980**, *36*, 275.
(14) Bykov, G. A.; Hien, Pham Zuy. *Zh. Eksp. Teor. Fiz.* **1962**, *43*, 909.

0020-1669/84/1323-1241$01.50/0

variation of the Fe–Cl bond is minor (viz. 0.03 Å), the total cell volume change between 295 and 130 K being about 8%. It has been noted, in this study, that the low-temperature structure is suggestive of disorder of the acetone molecules within the lattice.

In the following, we report the results of a detailed analysis of the high-spin ($^5T_2$) ⇌ low-spin ($^1A_1$) transition in [Fe(dppen)$_2$Cl$_2$]·2(CH$_3$)$_2$CO based on ^{57}Fe Mössbauer-effect and X-ray powder diffraction measurements, as a function of temperature. Moreover, evidence for an order–disorder transition of the acetone and its relation to the spin transition of the compound is reported.

Experimental Section

Materials. The sample of dichlorobis[*cis*-1,2-bis(diphenylphosphino)ethylene]iron(II)–acetone (1/2), [Fe(dppen)$_2$Cl$_2$]·2(CH$_3$)$_2$CO, was prepared as described elsewhere.[10] The sample gave satisfactory analyses, its physical data being in agreement with those reported previously.

Methods. ^{57}Fe Mössbauer spectra were measured with a spectrometer consisting of a constant-acceleration electromechanical drive and a Canberra 8100 multichannel analyzer operating in the multiscaling mode. A 50-mCi source of ^{57}Co in rhodium was used, the calibration being effected with a 25-μm metallic iron absorber. All velocity scales and isomer shfts are referred to the iron standard at 298 K. For conversion to the sodium nitroprusside scale, add +0.257 mm s^{-1}. Variable-temperature measurements were performed by using a custom-made superinsulated cryostat, the temperature being monitored by means of a calibrated iron vs. constantan thermocouple and a cryogenic temperature controller (Thor Cryogenics Model E 3010-II). The relative accuracy of temperature reading was about 0.05 K, and the absolute accuracy was about 0.5 K. The Mössbauer spectra were fitted to Lorentzian line shapes with use of a least-squares procedure. In the computer program, positions, line widths, and intensities of the individual peaks were treated as independent parameters, except where the contribution by one of the constituents was very small. In this case, a constraint was applied to the width and, if required, to the intensity for the two peaks of the particular constituent.

The effective thickness t_i corresponding to each individual line of the spectra was obtained from the background-corrected normalized area[14,15]

$$A_i = \tfrac{1}{2}\pi f_S \Gamma_i [L(t_i)] \quad (1)$$

In eq 1, f_S is the Debye–Waller factor of the source, Γ_i is the line width of the absorber (in the present case, it is $\Gamma_i = \Gamma_0$, where Γ_0 is the natural line width), and $L(t_i)$ is the saturation function. Employing the approximation $L(t_i) \approx t_i/(1 + 0.25t_i)$, which holds for $0 \le t_i \le 2$ with an accuracy better than 1%, one obtains

$$t_i = 1/[(\pi f_S \Gamma_i / A_i) - 0.25] \quad (2)$$

The effective thickness for one of the spin constituents, i.e. $t_{^5T_2}$ or $t_{^1A_1}$, is then obtained by addition of the corresponding values for the individual peaks, t_i.

Measurements of X-ray powder diffraction were performed with a Siemens counter diffractometer equipped with an Oxford Instruments CF 108A flow cryostat. Cu Kα radiation was used. Measurements of peak profiles were carried out between 130 and 300 K for each 5 K temperature change in the mode of step scanning of the apparatus, the steps being 0.02° for 2θ values between 7 and 27°. The resulting pulses were stored in a multichannel analyzer (Elscint MEDA 10). To obtain accurate values for the peak positions, the intense lines were least-squares fitted in terms of Gaussian line shapes. Temperatures were measured by a calibrated resistance thermometer, the relative accuracy being about 0.1 K. It was verified that the acetone of crystallization was not lost to any measurable extent during the evacuation of the flow cryostat.

Results

^{57}Fe Mössbauer Effect. Temperature Dependence of Quadrupole Splitting and Isomer Shift. Samples of [Fe(dppen)$_2$Cl$_2$]·2(CH$_3$)$_2$CO have been studied by ^{57}Fe Mössbauer spectroscopy between 85.4 and 307.2 K. Figure 1 shows five typical spectra, i.e. those for 182.7, 235.2, 241.8, 250.1, and 297.0 K, selected from an increasing-temperature series of measurements. The intense doublet in the spectrum of 182.7 K is characterized by the quadrupole splitting $\Delta E_Q = 0.64 \pm 0.01$ mm s^{-1} and the isomer shift $\delta^{IS} = 0.45 \pm 0.01$ mm s^{-1}. On the basis of these parameter values, the doublet is assigned to the low-spin $^1A_1$ ground state of iron(II). At 235.2 K, a second doublet is clearly visible, the corresponding Mössbauer parameters being $\Delta E_Q = 2.62 \pm 0.01$ mm s^{-1} and $\delta^{IS} = 0.82 \pm 0.01$ mm s^{-1}. This doublet is assigned to the high-spin $^5T_2$ ground state of iron(II). If the temperature is increased further, the high-spin doublet gains intensity, while the intensity of the low-spin doublet is simultaneously decreasing (cf. spectra at 241.8 and 250.1 K). At 297.0 K, only the high-spin spectrum is observed, whereby $\Delta E_Q = 2.54 \pm 0.01$ mm s^{-1} and $\delta^{IS} = 0.80 \pm 0.01$ mm s^{-1}. From these observations it is evident that the high-spin ($^5T_2$) ⇌ low-spin ($^1A_1$) transition in [Fe(dppen)$_2$Cl$_2$]·2(CH$_3$)$_2$CO is of continuous character. At 182.7 K, a very small contribution (~4%) of the high-spin spectrum is visible, the Mössbauer spectra remaining almost unchanged below that temperature. The transition is therefore incomplete at the low-temperature end, although the residual high-spin fraction is only around 0.03. In contrast, the transition achieves completion toward the high temperatures at ~281.2 K. Detailed values of the Mössbauer parameters for a representative number of temperatures are listed in Table I.

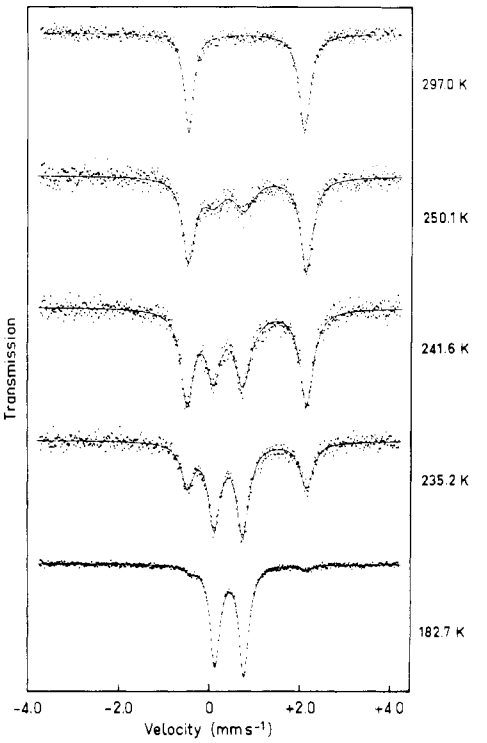

Figure 1. ^{57}Fe Mössbauer-effect spectra of [Fe(dppen)$_2$Cl$_2$]·2(CH$_3$)$_2$CO at 182.7, 235.2, 241.6, 250.1, and 297.0 K for increasing temperature series of measurements. The transition is centered at $T_c \simeq 240$ K. The transmission scales of the individual spectra are different.

The spectra have been collected for both increasing and decreasing temperatures under identical geometry of the source, absorber, and detector, and no hysteresis effects have been observed. From Figure 1 it is evident that, at 241.8 K, the intensity of the two doublets is comparable in magnitude. Indeed, as will be seen below, the spin transition is centered close to this temperature. Moreover, it may be noted that, at this temperature, the line width of both doublets is significantly larger than at temperatures where the system is in

(15) Lang, G. *Nucl. Instrum. Methods* **1963**, *24*, 425.

Table I. ^{57}Fe Mössbauer-Effect Parameters for $[Fe(dppen)_2Cl_2]\cdot 2(CH_3)_2CO$ for a Representative Set of Temperatures[a]

T, K	$\Delta E_Q(^1A_1)$,[b] mm s^{-1}	$\delta^{IS}(^1A_1)$,[c] mm s^{-1}	$\Delta E_Q(^5T_2)$,[b] mm s^{-1}	$\delta^{IS}(^5T_2)$,[c] mm s^{-1}	$t_{^5T_2}/t_{total}$
85.4	0.67	+0.47	2.63 ± 0.04	+0.89 ± 0.03	0.03
133.4	0.65	+0.46	2.57 ± 0.04	+0.86 ± 0.03	0.04
182.7	0.64	+0.45	2.57 ± 0.04	+0.86 ± 0.03	0.04
209.8	0.64	+0.45	2.62 ± 0.04	+0.83 ± 0.03	0.06
219.4	0.62	+0.44	2.62 ± 0.03	+0.84 ± 0.02	0.11
226.8	0.62	+0.43	2.60 ± 0.02	+0.84 ± 0.02	0.16
232.1	0.63	+0.43	2.61	+0.84	0.23
235.2	0.63	+0.42	2.62	+0.82	0.34
238.2	0.64	+0.42	2.62	+0.83	0.44
241.8	0.66	+0.41	2.63	+0.82	0.53
244.3	0.66 ± 0.02	+0.43 ± 0.02	2.61	+0.81	0.58
247.3	0.69 ± 0.03	+0.41 ± 0.02	2.62	+0.82	0.65
250.1	0.68 ± 0.04	+0.42 ± 0.03	2.60	+0.83	0.67
252.4	0.72 ± 0.04	+0.41 ± 0.03	2.61	+0.83	0.70
262.8			2.58	+0.82	0.79
271.4			2.56	+0.82	0.89
281.2			2.55	+0.81	1.00
297.0			2.54	+0.80	1.00
307.2			2.55	+0.78	1.00

[a] The data presented have been obtained for increasing temperatures. For decreasing temperatures, almost identical data have been obtained. [b] The experimental uncertainty is ±0.01 mm s^{-1}, except where stated. [c] Isomer shifts δ^{IS} are listed relative to iron metal at 298 K. The experimental uncertainty is ±0.01 mm s^{-1}, except where stated.

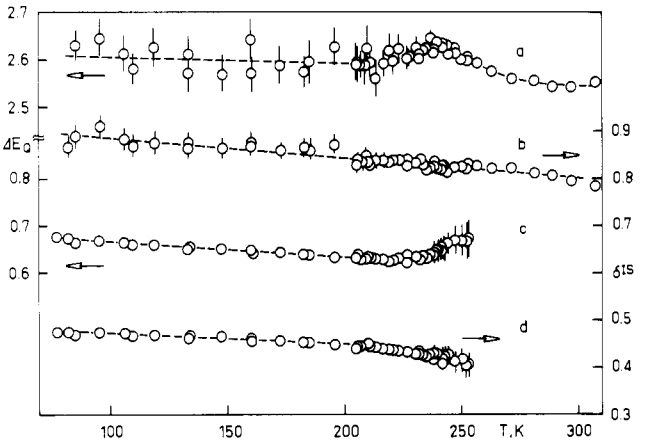

Figure 2. Temperature dependence of the Mössbauer-effect parameters of $[Fe(dppen)_2Cl_2]\cdot 2(CH_3)_2CO$ for the high-spin $^5T_2$ ground state $\Delta E_Q(^5T_2)$ (a) and $\delta^{IS}(^5T_2)$ (b) and the low-spin $^1A_1$ ground state $\Delta E_Q(^1A_1)$ (c) and $\delta^{IS}(^1A_1)$ (d). Fitting errors are marked only where larger than the size of the notation. Dashed lines are drawn by inspection. Data originate from two sets of measurements for the same absorber.

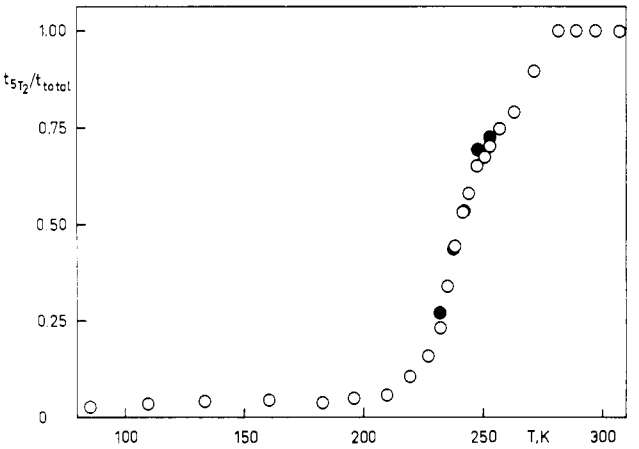

Figure 3. Temperature dependence of the relative effective thickness for the $^5T_2$ constituent, $t_{^5T_2}/t_{total}$, for increasing (○) and decreasing (●) temperature measurements.

either one of the two spin states. This finding will be discussed in more detail in the next section.

In Figure 2, the values of the quadrupole splitting and the isomer shift are plotted, as a function of temperature, for the two spin states of $[Fe(dppen)_2Cl_2]\cdot 2(CH_3)_2CO$. Evidently, there is a maximum in the values of $\Delta E_Q(^5T_2)$ in the spin transition region, i.e. at ~238 K. Although the error in the estimation of $\Delta E_Q(^5T_2)$ for the residual $^5T_2$ fraction, i.e. below ~220 K, is relatively large due to the small $^5T_2$ contribution, the observed maximum is definitely outside the experimental uncertainty. For the $^1A_1$ constituent, there is a clear deviation of $\Delta E_Q(^1A_1)$ from the smooth curve toward higher values as the spin transition initiates, *i.e.* again at ~238 K. The values of $\delta^{IS}(^5T_2)$ are somewhat low in comparison to the values observed for iron(II) complexes of the $[Fe^{II}N_6]$ type. The relatively low values are typical for highly covalent $^5T_2$ ground states of iron(II) and may be related to electronegativity and geometry of the phosphine ligand. No detectable discontinuity in the values of $\delta^{IS}(^5T_2)$ has been observed in the spin transition region. The values of $\delta^{IS}(^1A_1)$ are in the range normally found for the low-spin $^1A_1$ state of iron(II), a slight decrease of $\delta^{IS}(^1A_1)$ being apparent in the spin transition region. The dashed straight lines drawn through the δ^{IS} values for the two spin constituents show a slight variation in their temperature dependence that is arising due to the difference in second-order Doppler shift. The estimated values for their slope are $\partial(\delta^{IS}(^5T_2))/\partial T \approx -0.000\,43$ mm s^{-1} K^{-1} (between 80 and 300 K) and $\partial(\delta^{IS}(^1A_1))/\partial T \approx -0.000\,23$ mm s^{-1} K^{-1} for the region where there is no deviation from the linear behavior (between 80 and 200 K). This difference in the values of $\partial(\delta^{IS})/\partial T$ is consistent with different values for the Debye–Waller factors of the two spin constituents.

Quantities Derived from Mössbauer-Effect Areas. Temperature Dependence of Total Effective Thickness and Line Width. Following the procedure outlined in the Experimental Section, we have determined the effective thickness t_i, i = $^5T_2$, $^1A_1$, for the two ground states, individually. In Figure 3, the relative effective thickness for the $^5T_2$ state, $t_{^5T_2}/t_{total}$, is displayed as a function of temperature as derived from both increasing and decreasing temperature measurements. It is evident that no thermal hysteresis is observed. From the figure it may be also seen that, unlike the results of previous studies,[7,8] the temperature dependence of $t_{^5T_2}/t_{total}$ is not a continuous curve but rather shows a small inflection at ~250 K, which will be discussed below. It should be noted that the quantity $t_{^5T_2}/t_{total}$ represents the high-spin fraction $n_{^5T_2}$ except for the difference in the recoil-free fraction of the two spin constitu-

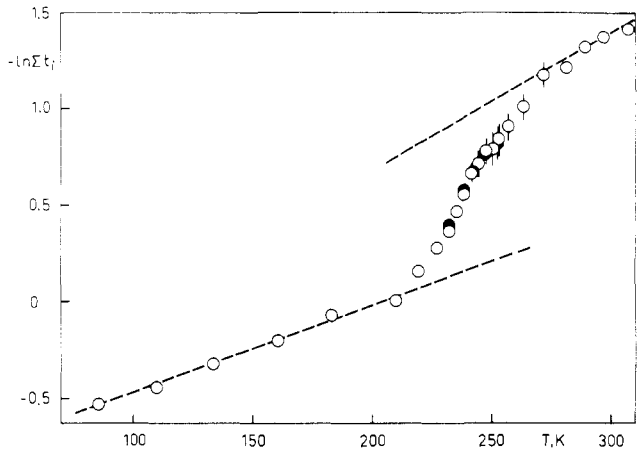

Figure 4. Temperature dependence of the quantity $-\ln(\sum t_i)$, where i = $^5T_2$, $^1A_1$ and t_i is the effective thickness, on the basis of ^{57}Fe Mössbauer-effect measurements for $[Fe(dppen)_2Cl_2]\cdot 2(CH_3)_2CO$. Measurements are for both increasing (○) and decreasing (●) temperatures. The error bars are marked only where larger than the size of notation. Errors represent the sum of fitting uncertainties for all four peaks.

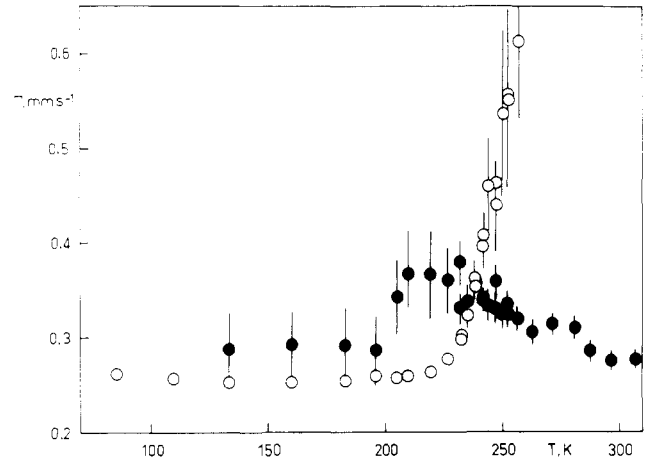

Figure 5. Temperature dependence of the observed line width Γ from Mössbauer-effect measurements on $[Fe(dppen)_2Cl_2]\cdot 2(CH_3)_2CO$: (●) high-spin $^5T_2$ ground state; (○) low-spin $^1A_1$ ground state. Error bars are marked only where larger than the size of notation.

ents. The transition temperature T_c is usually defined as the temperature where $n_{^5T_2} = 0.50$. Apart from the mentioned difference, the results of Figure 3 therefore show that $T_c \simeq$ 240 K.

On the basis of a single set of measurements that were recorded under identical geometrical conditions, the quantity $-\ln(\sum t_i)$is displayed, in Figure 4, as a function of temperature. The curve represents the behavior of the total Debye–Waller factor of the system. In regions sufficiently distant from the transition temperature T_c, the behavior of $-\ln(\sum t_i)$ is approximated by the indicated straight lines. It is evident that the Debye–Waller factors for the two spin states are significantly different. The characteristic Mössbauer temperatures have been estimated from the slope of the two lines as $\Theta^M_{^5T_2}$ = 138 K and $\Theta^M_{^1A_1}$ = 173 K. The detailed determination of the recoil-free fractions $f_{^5T_2}$ and $f_{^1A_1}$ for molecular compounds can be performed only under certain simplifying assumptions, which were discussed elsewhere,[7] although, on a qualitative basis, it can be concluded that $f_{^1A_1} > f_{^5T_2}$. Similar to the finding for $t_{^5T_2}/t_{total}$ (cf. Figure 3), there is a slight inflection of the $-\ln(\sum t_i)$ curve at ~250 K.

In Figure 5, the average line widths at half-height have been plotted for the two spin constituents of $[Fe(dppen)_2Cl_2]\cdot 2(CH_3)_2CO$. From the figure it is seen that there is an unusual

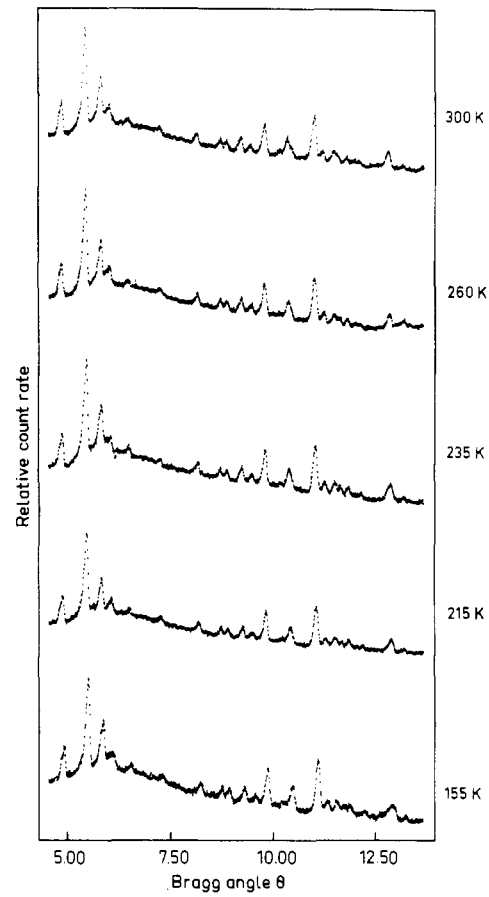

Figure 6. X-ray powder diffraction patterns for $[Fe(dppen)_2Cl_2]\cdot 2(CH_3)_2CO$ at the temperatures of 155, 215, 235, 260, and 300 K.

increase of the line width for the low-spin constituent $\Gamma_{^1A_1}$ as the transition proceeds. Similarly, a noticeable increase in the values of $\Gamma_{^5T_2}$ is observed within the spin transition region, although the absolute change is considerably smaller. As the transition proceeds, the uncertainty in the estimation of the line width of the minority constituent is increasing and thus the errors are increasing correspondingly. The observed variation of both $\Gamma_{^1A_1}$ and $\Gamma_{^5T_2}$ is significantly different from that of other systems involved in a continuous high-spin ($^5T_2$) ⇌ low-spin ($^1A_1$) transition.[7,8]

X-ray Powder Diffraction. Temperature Dependence of Lattice Spacings. X-ray powder diffraction patterns have been recorded for $[Fe(dppen)_2Cl_2]\cdot 2(CH_3)_2CO$ over the range of the diffraction angle $3.5° \leq \theta \leq 13.5°$ at various temperatures. A selection of the results is displayed in Figure 6. The patterns at 155 and 300 K correspond to the situations where the system is almost completely in one of the spin states, low-spin $^1A_1$ and high-spin $^5T_2$, respectively, whereas at 235 K, the two spin constituents are of approximately equal abundance. The two other temperatures, i.e. 215 and 260 K, are characterized by the initiation and the completion of the spin transition, and thus one of the spin constituents is predominant with respect to the other. From a comparison of the patterns it is immediately evident that, in contrast to the observation for discontinuous transitions,[3-6] no new peaks emerge in the spin transition region. Moreover, even the relative intensities of all the lines remain almost invariant. There is a systematic shift of the peak positions in the spin transition region which may be followed, for example, for the two lines that are observed at the diffraction angles θ = 9.45° (line I) and θ = 10.67° (line II) for 155 K. Evidently, line I shifts to 9.36° for 300 K, whereas line II is displaced to 10.57°. The results have been employed to estimate the values of lattice spacings d_{hkl} for the two selected Bragg reflections, their temperature

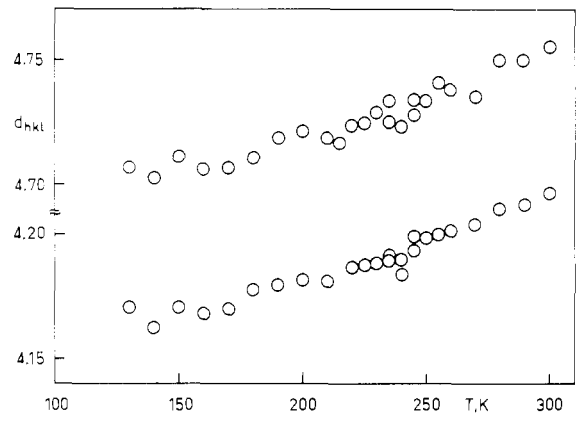

Figure 7. Temperature dependence of lattice spacings d_{hkl} for two intense Bragg reflections of $[Fe(dppen)_2Cl_2]\cdot 2(CH_3)_2CO$ at $\theta = 9.36°$ and $\theta = 10.57°$ (for 300 K).

dependence being shown in Figure 7. There is some variation of d_{hkl} values due to experimental uncertainties. The observed temperature dependence of diffraction angles and thus lattice spacings for the intense diffraction lines is nonetheless clearly established and should be most likely attributed to the volume expansion associated with the high-spin ($^5T_2$) $\rightleftharpoons$ low-spin ($^1A_1$) transition.

Discussion

The Continuous High-Spin ($^5T_2$) $\rightleftharpoons$ Low-Spin ($^1A_1$) Transition. In contrast to a number of spin transitions that have been established as first order,[3-6,16-18] the high-spin ($^5T_2$) $\rightleftharpoons$ low-spin ($^1A_1$) transition studied at present may be described in terms of a continuous change with temperature of such physical properties as the effective magnetic moment,[10] the $^5T_2$ fraction derived from the ^{57}Fe Mössbauer effect (albeit only the quantity $t_{^5T_2}/t_{total}$ has been presented in Figure 3), and the lattice spacings d_{hkl} derived from X-ray powder diffraction. No hysteresis effects have been observed for any of these quantities. The residual fraction of the $^5T_2$ state at low temperatures is about 0.03, and that of the $^1A_1$ state at high temperatures is close to zero, the transition being almost complete at both temperature ends. $[Fe(dppen)_2Cl_2]\cdot 2(CH_3)_2CO$ may be therefore considered as an example of a spin transition of the continuous type. This is analogous to the compounds $[Fe(bts)_2(NCS)_2]$[7] and $[Fe(4\text{-}paptH)_2]X_2\cdot 2H_2O$, X = ClO_4, BF_4,[8] which have been studied previously.

A particularly striking result of the present study is provided by the observed temperature dependence of $-\ln(\sum t_i)$ (cf. Figure 4). The significant difference in the slope of this curve at temperatures sufficiently away from the spin transition region clearly establishes the different Debye–Waller factors of the two spin isomers. The different Debye–Waller factors are a consequence of the variation of Fe–P bond distances[10] and possibly some additional changes in the geometry of the $[Fe(dppen)_2Cl_2]$ molecules on spin transition. Similar changes of Fe–N bond lengths have been reported previously for a number of systems involved in a high-spin ($^5T_2$) $\rightleftharpoons$ low-spin ($^1A_1$) transition.[11-13] In general, these changes are associated with a variation of the corresponding vibrational frequencies. From the results of X-ray diffraction measurements reported above, it follows that the two spin isomers of $[Fe(dppen)_2Cl_2]$ are almost randomly distributed within the *same* lattice. Therefore, the intermolecular vibrations are expected to be similar, whereas intramolecular vibrations may be different.[19-21] The nonlinear dependence of $-\ln(\sum t_i)$ on temperature therefore represents the effect of the variation of the intramolecular vibrations on the recoil-free fraction.

The observed difference in the temperature factor of the isomer shift is another consequence of the change of the Fe–P bond distance on spin transition. It is well-known that the temperature-dependent contribution to the isomer shift is due to second-order Doppler effect, the latter being directly related to the Debye–Waller factor.[22] The observed variation in the values of $\partial(\delta^{IS})/\partial T$ therefore provides an independent support for the different Debye–Waller factors of the two spin constituents.

Of considerable importance is the fact that, in X-ray powder diffraction, only a continuous shift of peak positions or lattice spacings with temperature is observed (cf. Figures 6 and 7). This finding is very similar to the observations reported earlier for $[Fe(bts)_2(NCS)_2]$[7] and $[Fe(4\text{-}paptH)_2]X_2\cdot 2H_2O$, X = ClO_4, BF_4,[8] and is in sharp contrast to the results obtained for spin transitions of the discontinuous type. In that case, individual diffraction patterns for the two spin phases, high-spin $^5T_2$ and low-spin $^1A_1$, are observed, their intensities varying with the temperature.[3-6] It has been pointed out previously[7,8] that a single X-ray diffraction pattern will be indeed expected if a *random* distribution of the two spin isomers within the *same* lattice is assumed. The distribution of the two spin constituents thus determines the macroscopic type, *i.e* discontinuous or continuous, which the spin transition assumes. A wide distribution of the minority constituent will produce a single X-ray diffraction pattern and will be associated with a transition of the continuous type, whereas a narrow distribution of the two phases that results in pronounced domain formation will produce different diffraction patterns for the two phases and will give rise to a discontinuous type of transition.

The fact that the lattice spacings of Figure 7 do not follow in detail the expected behavior of the $^5T_2$ fraction with temperature is not in conflict with the above conclusions, since this variation depends on the choice of reflections.

The results obtained for the spin transition in $[Fe(dppen)_2Cl_2]\cdot 2(CH_3)_2CO$ thus show that the two constituents, high-spin $^5T_2$ and low-spin $^1A_1$, show a behavior that is closely related to that of a solid solution of two components.

Order–Disorder Transition of the Acetone Molecules and Its Effect on the ^{57}Fe Mössbauer Spectra. In the Mössbauer effect, a slight resolution of the high-spin $^5T_2$ spectrum into two doublets was noted in the spin transition region. This feature was clearly apparent in the original spectra and may be visualized here on the basis of an unusual increase of the line width (cf. Figure 5). If the transition is approached from the high temperatures, the line width for the $^5T_2$ doublet increases from a normal value of $\Gamma_{^5T_2} \simeq 0.29$ mm s^{-1} to a maximum of $\Gamma_{^5T_2} \simeq 0.40$ mm s^{-1} at 232 K. Below T_c, a decrease of the line width sets in. It should be noted however that, at e.g. 209.8 K, the $^5T_2$ fraction is only $\sim$6% with a correspondingly large margin of error for $\Gamma_{^5T_2}$. At low temperatures, the line width for the $^1A_1$ doublet is $\Gamma_{^1A_1} \simeq 0.26$ mm s^{-1} and these values start to increase as the transition is approached until a maximum value $\Gamma_{^1A_1} \simeq 0.55$ mm s^{-1} is achieved at $\sim$256 K. Above this temperature, the low-spin doublet cannot be observed. The increase in line width is highly unusual and is attributed to the unresolved doubling of the Mössbauer spectrum mentioned above. This behavior bears a close resemblance to observations associated with the order–disorder transition of the perchlorate anion in $[Fe(bi)_3](ClO_4)_2$, where

(16) König, E.; Ritter, G. *Solid State Commun.* **1976**, *18*, 279.
(17) Ritter, G.; König, E.; Irler, W.; Goodwin, H. A. *Inorg. Chem.* **1978**, *17*, 224.
(18) Sorai, M.; Ensling, J.; Hasselbach, K. M.; Gütlich, P. *Chem. Phys.* **1977**, *20*, 197.
(19) König, E.; Madeja, K. *Spectrochim. Acta, Part A* **1967**, *23A*, 45.
(20) Takemoto, J. H.; Hutchinson, B. *Inorg. Nucl. Chem. Lett.* **1972**, *8*, 769.
(21) Takemoto, J. M.; Hutchinson, B. *Inorg. Chem.* **1973**, *12*, 705.
(22) Taylor, R. D.; Craig, P. P. *Phys. Rev.* **1968**, *175*, 782.

bi = 2,2′-bi-2-imidazoline.[6] In this compound, the transition produces a doubling of the high-spin $^5T_2$ lines in the ^{57}Fe Mössbauer spectrum at temperatures lower than the transition temperature $T_c^{ClO_4} \simeq 199$ K. At $T_c^{ClO_4}$, the disorder of the ClO_4 anions is apparently frozen out, each perchlorate assuming one or the other of two possible configurations.

It is therefore suggested that the acetone molecules in $[Fe(dppen)_2Cl_2]\cdot 2(CH_3)_2CO$ are involved in an order–disorder transition centered at $T_c^{acetone} \simeq 240$ K. The transition will result in slight changes of the Fe–P ligation with a consequent effect on the iron sites. In this case, two separate high-spin $^5T_2$ doublets would be expected in the Mössbauer spectrum at $T < T_c^{acetone}$, which should collapse into a single $^5T_2$ doublet above $T_c^{acetone}$. This assumption is fully consistent with the observed broadening of line width discussed above. The conclusion is further supported by the inflection of the effective thickness $t_{s_{T_2}}/t_{total}$ (cf. Figure 3) and the change in slope of the quantity $-\ln(\sum t_i)$ (cf. Figure 4) at that temperature. The maximum in the temperature function of the quadrupole splitting $\Delta E_Q(^5T_2)$ is also found at ~240 K as is the increase of the values for $\Delta E_Q(^1A_1)$ (cf. Figure 2). Since there is no marked change in X-ray diffraction in the region of 240 K, a phase transition at that temperature is ruled out. The suggested order–disorder transition thus should be second or higher order. It is important to note that, in the X-ray structure investigation of the low-spin isomer of $[Fe(dppen)_2Cl_2]\cdot 2(CH_3)_2CO$ at 130 K, ΔF maps show that the acetone molecule is almost equally distributed between two different orientations.[10] The two slightly different iron sites observed in the Mössbauer effect below $T_c^{acetone}$ thus correspond to two different orientations of the acetone molecule. In $[Fe(bi)_3](ClO_4)_2$, the order–disorder transition at $T_c^{ClO_4} \simeq 199$ K and the high-spin ($^5T_2$) $\rightleftharpoons$ low-spin ($^1A_1$) transition at $T_c^{\uparrow} = 114.8$ K (for increasing temperatures) are well separated and are of abrupt character.[6] In the present compound, both the order–disorder transition of the acetone and the spin transition seem to be centered at almost the same temperature and are of a gradual nature. It is therefore very likely that, as the temperature is lowered in the region of the high-spin isomer, the orientationally disordered acetone molecules gradually tend to arrange regularly and thus the order–disorder transition triggers the spin transition that sets in at about 270 K. A similar mechanism has been proposed for the high-spin ($^5T_2$) $\rightleftharpoons$ low-spin ($^1A_1$) transition in $[Fe(2\text{-pic})_3]Cl_2\cdot C_2H_5OH$, where 2-pic = 2-picolylamine.[13] In this compound, the ethanol molecules are hydrogen bonded to the Cl anions and exhibit orientational disorder in the high-spin state, whereas a regular arrangement is observed in the low-spin state. As the spin transition and the order–disorder transition of the ethanol molecule set in, the complex and the ethanol interact through hydrogen bonds. It should be noted that in both $[Fe(dppen)_2X_2]\cdot 2(CH_3)_2CO$, X = Cl, Br, and $[Fe(2\text{-pic})_3]Br_2\cdot C_2H_5OH$ the continuous transition is relatively sharp and almost complete at both temperature ends, whereas if the solvent, acetone or ethanol, is removed from the lattice, the spin transition becomes very gradual and incomplete at low as well as high temperatures.[9,10,23] This suggests that, in the present compound, intermolecular interactions between the complex and the solvent molecule are important and possibly assist in the propagation of the spin transition through the lattice.

Acknowledgment. We appreciate financial support by the Deutsche Forschungsgemeinschaft and the Fonds der Chemischen Industrie.

Registry No. $Fe(dppen)_2Cl_2$, 58031-48-4.

(23) Greenaway, A. M.; O'Connor, C. J.; Schrock, A.; Sinn, E. *Inorg. Chem.* **1979**, *18*, 2692.

Contribution from the Department of Chemistry, University of Alberta, Edmonton, Alberta, Canada T6G 2G2

Nuclear Magnetic Resonance Studies of the Solution Chemistry of Metal Complexes. 20. Ligand-Exchange Kinetics of Methylmercury(II)–Thiol Complexes

DALLAS L. RABENSTEIN* and R. STEPHEN REID

Received June 20, 1983

The kinetics of the exchange of methylmercury, CH_3Hg^{II}, between thiol ligands in aqueous solution was studied by ^1H NMR spectroscopy over a range of pH values. Exchange of CH_3Hg^{II} between two different mercaptoacetic acid ligands and between mercaptoacetic acid and cysteine, penicillamine, or glutathione was found to be by displacement of complexed thiol by free thiol at pH >1. The exchange rate is pH dependent due to the effect of protonation of the ligand. For the amino acid and peptide ligands, exchange at physiological pH is predominantly via displacement of complexed mercaptoacetic acid by the amino-protonated, thiol-deprotonated form of the displacing ligand. At pH <1, exchange is predominantly via proton-assisted dissociation of the complex followed by reaction of CH_3Hg^{II} with free thiol. The second-order rate constants for displacement of complexed thiol by free thiol are consistent with an associative mechanism, in which the exchange rate constant is determined by the free energy difference between the two complexes.

Introduction

The mechanism by which the methylmercury cation, CH_3Hg^{II}, is exchanged between thiol ligands is of both chemical and biological interest. CH_3Hg^{II}–thiol complexes are very stable thermodynamically, having formation constants in the 10^{15}–10^{17} range.[1-4] However, they are very labile, as indicated by the observation of exchange-averaged resonances in ^1H and ^{13}C NMR spectra for thiol ligands in solutions containing CH_3Hg^{II} and an excess of thiol.[3-7] CH_3Hg^{II} is also apparently quite labile in biological systems, exchanging among the multitude of thiol ligands it encounters, with some ultimately combining with thiol ligands in the central nervous system.[8] Consistent with this, exchange-averaged ^1H reso-

(1) Schwarzenbach, G.; Schellenberg, M. *Helv. Chim. Acta* **1967**, *48*, 28.
(2) Simpson, R. B. *J. Am. Chem. Soc.* **1961**, *83*, 4717.
(3) Reid, R. S.; Rabenstein, D. L. *Can. J. Chem.* **1981**, *59*, 1505.
(4) Reid, R. S.; Rabenstein, D. L. *J. Am. Chem. Soc.* **1982**, *104*, 6733.
(5) Rabenstein, D. L.; Fairhurst, M. T. *J. Am. Chem. Soc.* **1975**, *97*, 2086.
(6) Bach, R. D.; Weibel, A. T. *J. Am. Chem. Soc.* **1976**, *98*, 6241.
(7) Rabenstein, D. L.; Evans, C. A. *Bioinorg. Chem.* **1978**, *8*, 107.

0020-1669/84/1323-1246$01.50/0